Article

Hierarchical Assembly of Two-Dimensional Homochiral Nanocavity Arrays

Hannes Spillmann, Alexandre Dmitriev, Nian Lin, Paolo Messina, Johannes V. Barth, and Klaus Kern

J. Am. Chem. Soc., **2003**, 125 (35), 10725-10728• DOI: 10.1021/ja0362353 • Publication Date (Web): 08 August 2003

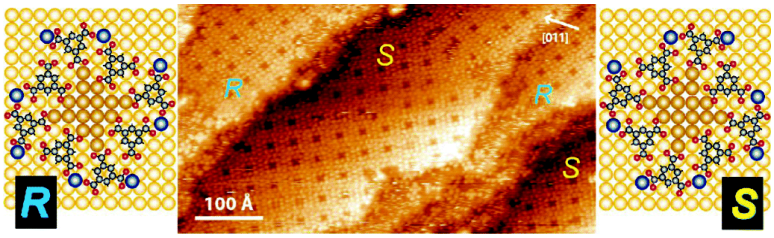

More About This Article

Additional resources and features associated with this article are available within the HTML version:

- Supporting Information
- Links to the 28 articles that cite this article, as of the time of this article download
- Access to high resolution figures
- Links to articles and content related to this article
- Copyright permission to reproduce figures and/or text from this article

View the Full Text HTML

J|A|C|S
ARTICLES
Published on Web 08/08/2003

Hierarchical Assembly of Two-Dimensional Homochiral Nanocavity Arrays

Hannes Spillmann,[†] Alexandre Dmitriev,[†] Nian Lin,*[,†] Paolo Messina,[†] Johannes V. Barth,*[,‡] and Klaus Kern[†,‡]

Contribution from the Max-Planck-Institut für Festkörperforschung, Heisenbergstrasse 1, D-70569 Stuttgart, Germany, and Institut de Physique des Nanostructures, Ecole Polytechnique Fédérale de Lausanne, CH-1015 Lausanne, Switzerland

Received May 20, 2003; E-mail: n.lin@fkf.mpg.de; johannes.barth@epfl.ch

Abstract: We demonstrate the rational design of nanoporous two-dimensional supramolecular structures by the hierarchical assembly of organic molecules and transition metal atoms at surfaces. Single-molecule level observations with scanning tunneling microscopy monitor the successive *aufbau* of structures with increasing complexity. From the primary components secondary mononuclear chiral complexes are formed, which represent antecedents for tertiary polynuclear metal−organic nanogrids. These nanogrids represent the constituents of the eventually evolving two-dimensional networks comprising homochiral nanocavity arrays. Our findings visualize the evolution of complex matter in an exemplary way: from per se achiral species via chiral intermediates to mesoscale dissymmetric structures.

Introduction

Organizational hierarchies are abundant in biological systems and biomaterials such as proteins, viruses, or biogenic crystals.[1] In a similar way distinct levels of structural hierarchies and complexity are encountered in artificial supramolecular systems stabilized by noncovalent chemical bonds.[2] An intriguing issue where our current understanding is rather limited concerns the *aufbau* of highly organized supramolecular architectures, i.e. the principles governing the transition between the primary (molecular) building blocks and the final mesoscale systems. The steering of the corresponding processes will be paramount for the development of novel supramolecular functional materials.[3] Particularly interesting are low-dimensional chiral assemblies in view of their intrinsic relation to the biological world[4] and their importance in heterogeneous asymmetric catalysis, chemical sensing, enantioselective antibody recognition, and host−guest chemistry.[5]

Here we report single-molecule level observations on the hierarchical assembly of homochiral nanocavity arrays at a metal surface. Scanning tunneling microscopy (STM) was employed to monitor how structures at distinct levels of complexity are formed and integrated in higher-order arrangements. Scheme 1 shows the key findings: The primary building blocks 1,3,5-tricarboxylic benzoic acid (trimesic acid, TMA) molecules and Fe atoms assemble in the form of secondary mononuclear chiral complexes, which are stabilized by metal−ligand interactions. The secondary complexes in turn are antecedents for tertiary polynuclear nanogrids representing the dissymmetric motifs that in a final stage are organized in mesoscale networks comprising a regular arrangement of homochiral nanocavities. These nanocavities present identically shaped ∼1 nm diameter hosts, equally spaced by 3.43 nm from each other and functionalized by eight carboxylate groups in a well-defined arrangement. The precise positioning of the molecules and the metal centers at the surface opens up new possibilities for the bottom-up fabrication of complex functional nanomaterials.

Results and Discussion

Our studies were conducted under ultrahigh vacuum conditions using an atomically clean Cu(100) surface. The procedures for deposition of TMA molecules and metal atoms as described

[†] Max-Planck-Institut für Festkörperforschung.

[‡] Institut de Physique des Nanostructures, Ecole Polytechnique Fédérale de Lausanne.

(1) (a) Tian, Z. R.;. Liu, J.; Voigt, J. A.; Mckenzie, B.; Xu, H. *Angew. Chem., Int. Ed.* **2003**, *42*, 414. (b) Cölfen, H.; Mann, S. *Angew. Chem., Int. Ed.* **2003**, *42*, 2350. (c) Varner, J. E., Ed. *Self-Assembling Architecture*; Alan R. Liss: New York, 1988. (d) Cann, A. J. *Principles of Molecular Virology*, Academic Press: San Diego, 2001.

(2) (a) Fyfe, M. C. T.; Stoddart, J. F. *Acc. Chem. Res.* **1997**, *30*, 393−401. (b) Seidel, S. R.; Stang, P. J. *Acc. Chem. Res.* **2002**, *35*, 972−983.

(3) (a) Lopes, W. A.; Jaeger, H. M. *Nature* **2001**, *414*, 735−738. (b) Trau, M.; Yao, N.; Kim, E.; Xia, Y.; Whitesides, G. M.; Aksay, I. A. *Nature* **1997**, *390*, 674−676. (c) Eddaoudi, M.; Kim, J.; Rosi, N.; Vodak, D.; Wachter, J.; O'Keefe, M.; Yaghi, O. M. *Science* **2002**, *295*, 469−472. (d) Lehn, J.-M. *Science* **2002**, *295*, 2400−2403. (e) Ikkala, O.; Brinke, G. T. *Science* **2002**, *295*, 2407−2409. (f) Reinhoudt, D. N.; Crego-Calama, M. *Science* **2002**, *295*, 2403−2407. (g) Hollingsworth, M. D. *Science* **2002**, *295*, 2410−2413. (h) Huang, Y.; Duan, X.; Wei, Q.; Lieber, C. M. *Science* **2001**, *291*, 630−633. (i) Hatzor, A.; Moav, T.; Cohen, H.; Matlis, S.; Libman, J.; Vaskevich, A.; Shanzer, A.; Rubinstein, I.. *J. Am. Chem. Soc.* **1998**, *120*, 13469−13477. (j) Yang, P.; Deng, T.; Zhao, D. Y.; Feng, P. Y.; Pine, D.; Chmelka, B. F.; Whitesides, G. M.; Stucky, G. D. *Science* **1998**, *282*, 2244−2246.

(4) Bonner, W. A. *Origin Life Evol. Biosph.* **1995**, *25*, 175.

(5) (a) Lorenzo, M. O.; Baddeley, C. J.; Muryn, C.; Raval, R. *Nature* **2000**, *404*, 376−379. (b) Blaser, H.-U. *Tetrahedron*: *Asymmetry* **1991**, *2*, 843−866. (c) Moulton, B.; Zaworotko, M. J. *Chem. Rev.* **2001**, *101*, 1629−1658. (d) Bowden, N.; Choi, I. S.; Grzybowski, B. A.; Whitesides, G. M. *J. Am. Chem. Soc.* **1999**, *121*, 5373−5391. (e) Rivera, J. M.; Martin, T.; Rebek. J. *Science* **1998**, *279*, 1021−1023. (f) Kühnle, A.; Linderoth, T. R.; Hammer, B.; Besenbacher, F. *Nature* **2002**, *415*, 891−893. (g) Kepert, C. J.; Prior, T. J.; Rosseinsky, J. *J. Am. Chem. Soc.* **2000**, *122*, 5158−5168. (h) Geva, M.; Frolow, F.; Eisenstein, M.; Addadi, L. *J. Am. Chem. Soc.* **2003**, *125*, 696−704. (i) Davis, M. E. *Nature* **2002**, *417*, 813−821. (j) Cui, Y.; Evans, O. R.; Ngo, H. L.; White, P. S.; Lin, W. *Angew. Chem., Int. Ed.* **2002**, *41*, 1159. (k) Seo, J. S.; Whang, D.; Lee, H.; Jun, S. I.; Oh, J.; Jeon, Y. J.; Kim, K. *Nature* **2000**, *404*, 982−986.

Scheme 1. *Aufbau* of Dissymmetric Supramolecular Motifs Mediated by Hierarchical Assembly of Simple Achiral Species[a]

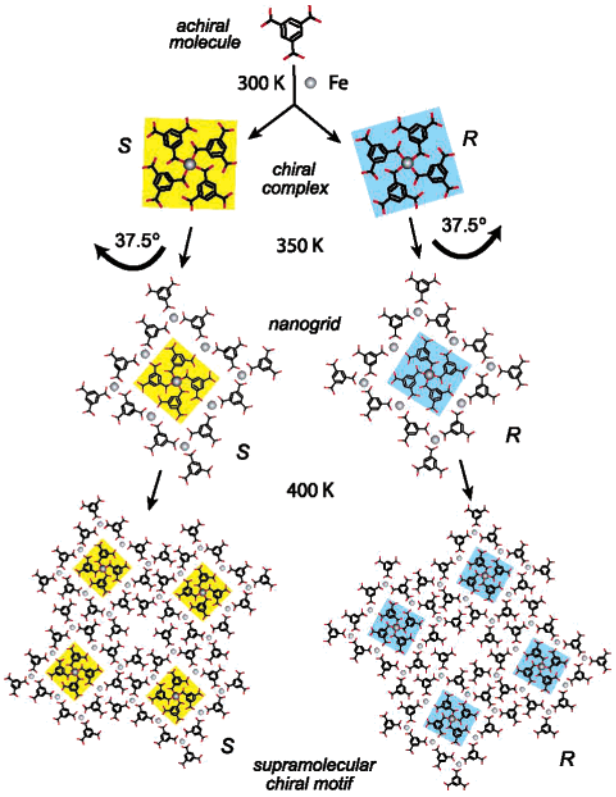

[a] 1,3,5-tricarboxylic benzoic acid (trimesic acid, TMA) molecules and Fe atoms represent the primary units which are employed for the formation of secondary chiral mononuclear ($Fe(TMA)_4$) complexes. The complexes are antecedents for tertiary polynuclear nanogrids which are in turn the supramolecular motifs for the assembly of homochiral nanocavity arrays. The respective mirror-symmetric configurations (labeled *S* and *R*) are indicated with yellow and turquoise background.

in the Experimental Section followed recipes outlined previously.[6−8] The employed substrate temperatures account for deprotonated carboxylic acid moieties of the TMA molecules, which lie flat on the surface and are resolved as equilateral triangles in STM data.[6] The molecules thus represent polytopic linkers with three exodentate functionalities. At 300 K the carboxylate ligands readily react with the coadsorbed Fe atoms, leading to the initial formation of cloverleaf-shaped $Fe(TMA)_4$ complexes where a central Fe atom is surrounded by four organic molecules.[7] While these mononuclear secondary structures consist of per se achiral building blocks, they are encountered in two mirror-symmetric configurations as demonstrated in Figure 1a. The reason underlying the chiral arrangement is the linkage of the molecules' symmetric bidentate COO ligands to the metal atom (representing the stereogenic center) in an organized unidentate fashion according to Scheme 1 (see ref 7 for a detailed discussion). Since *R* and *S* enantiomers are homogeneously distributed at the surface, this "cloverleaf phase" represents a racemic mixture. A further, albeit metastable, type of secondary structure is a Y-shaped complex made out

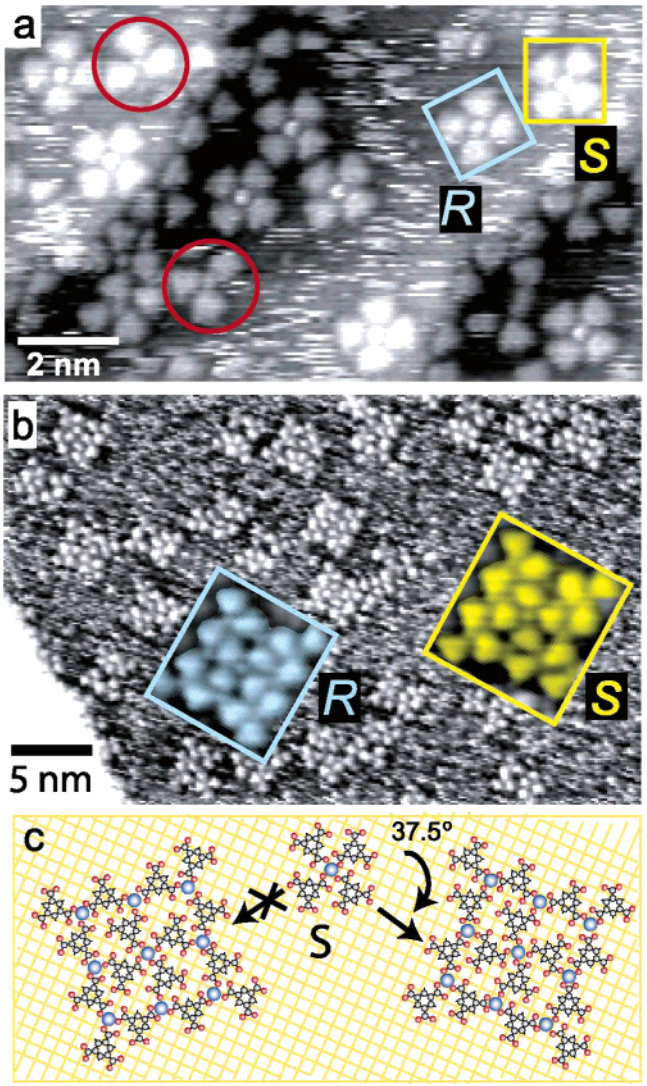

Figure 1. Hierarchical assembly of metal−organic architectures monitored by STM. (a) Secondary structures formed at 300 K. Color squares indicate two different enantiomers of cloverleaf-shaped $Fe(TMA)_4$ complexes (color coding following Scheme 1). Red circles mark metastable Y-shaped $Fe(TMA)_3$ complexes. (Fe coverage: 0.06 ML; TMA coverage: 0.8 ML.) (b) Assembly of tertiary stage: square-shaped polynuclear nanogrids evolve upon annealing at 350 K. The insets reveal that the respective core units of the dissymmetric metal−organic motifs are related to the chiral secondary $Fe(TMA)_4$ compounds (color coding as in Scheme 1). (Fe coverage: 0.02 ML; TMA coverage: 0.4 ML.) (c) Assembly of ideal polynuclear *S* nanogrid based on STM topography. A 37.5° clockwise rotation of the $Fe(TMA)_4$ cloverleaf core unit is necessary to allow for hollow-site adsorption of all Fe atoms (dark blue) involved.

of a single Fe atom coordinating three TMA molecules (marked by the red circles in Figure 1a). In contrast to the stable and immobile cloverleaf-shaped $Fe(TMA)_4$ complexes, the Y-shaped complexes are unstable and very mobile at 300 K and can only be observed at appreciable coverages in the vicinity of $Fe(TMA)_4$ species or at step edges, where their lifetime is locally increased due to steric hindrance of decay and lateral motion.[6] This implies in particular that in addition to the material in the stable coordination compounds, freely moving iron atoms and TMA molecules are present at the surface.

The next level of structural complexity is achieved upon annealing of the cloverleaf phase to 350 K (in rare cases similar structures evolved even at room temperature; however, they could be systematically obtained only upon annealing). Poly-

(6) Lin, N.; Dmitriev, A.; Weckesser, J.; Barth, J. V.; Kern, K. *Angew. Chem., Int. Ed.* **2002**, *41*, 4779−4783.
(7) Messina, P.; Dmitriev, A.; Lin, N.; Spillmann, H.; Abel, M.; Barth, J. V.; Kern, K. *J. Am. Chem. Soc.* **2002**, *124*, 14000−14001.
(8) (a) Weckesser, J.; Vita, A. D.; Barth, J. V.; Cai, C.; Kern, K. *Phys. Rev. Lett.* **2001**, *87*, 096101. (b) Barth, J. V.; Weckesser, J.; Trimarchi, G.; Vladimirova, M.; De Vita, A.; Cai, C. Z.; Brune, H.; Gunter, P.; Kern, K. *J. Am. Chem. Soc.* **2002**, *124*, 7991−8000.

nuclear assemblies which typically consist of 16 TMA molecules arranged in square-like molecular 4 × 4 nanogrids (see Figure 1b) are formed. High-resolution STM images (e.g., Figure 1b insets) reveal that the core unit of each nanogrid is an $Fe(TMA)_4$ complex which is surrounded by four Y-shaped complexes. This configuration suggests that the mononuclear complexes in the cloverleaf phase represent antecedents for the nanogrids. In the simplest picture this can be viewed as resulting from an attachment of four Y-shaped complexes to the corners of a cloverleaf-shaped $Fe(TMA)_4$ complex. The attachment is mediated by the incorporation of further metal atoms forming a second coordination shell (cf. Scheme 1). Annealing increases the probability of the attachment, thus promoting nanogrid formation. A closer inspection of the data reveals that the central cloverleaf complexes are additionally rotated by an angle of 37.5° in the nanogrids' development whereby their chiral nature persists (the rotation must be clockwise for *S* and counterclockwise for *R* species, respectively). This rearrangement is associated with the easier positioning of second-shell Fe atoms at the energetically preferred substrate hollow sites (note that in an ideal tertiary nanogrid a total of nine Fe atoms are included, and the ratio between Fe atoms and TMA molecules is 9:16, thus exceeding the ideal ratio of 1:4 for formation of mononuclear complexes at small coverages;[7] nevertheless, second-shell Fe atoms seem to be missing in some cases). As shown in Figure 1c, for a hypothetical *S* nanogrid made from an *S* cloverleaf-shaped complex in an unrelaxed geometry without rotation (model at the left side) only the central Fe atom maintains a hollow-site position while the others adsorb at unfavorable bridge or top sites of the Cu(100) surface. The 37.5° clockwise rotation (for the *S* species) allows for the positioning of all Fe atoms at hollow sites. The chiral arrangement of the secondary core units induces dissymmetric tertiary nanogrids. That is, there is a chirality proliferation in the nanogrid assembly. Accordingly, no translation or rotation in two dimensions would allow for a superposition of the mirror-symmetric configurations labeled *R* or *S* as depicted in Scheme 1 and Figure 1. Similar to the mononuclear complexes in the cloverleaf phase the *R* and *S* nanogrids are found to be homogeneously distributed on the surface, forming a racemic mixture. It is expected that with 9 Fe atoms adsorbed at energetically favored hollow sites the surface diffusion barrier for transport of an entire nanogrid is significantly higher than that of mononuclear complexes.

The final stage of complexity at the mesoscopic scale is achieved upon further annealing the substrate to 400 K, leading to the formation of extended regular metal−organic superstructures. Possibly the anneal enables nanogrid migration to be instrumental in the assembly process. The STM image reproduced in Figure 2a depicts the corresponding two-dimensional coordination networks with a square unit cell of 3.43 nm × 3.43 nm comprising a regular arrangement of nanocavities. These structures belong to the p4 symmetry group, thus reflecting the symmetry of the substrate atomic lattice. The tertiary nanogrids are identified as the underlying supramolecular motifs. Accordingly a close inspection of the data (cf. inset in Figure 2a) reveals that the shape of the individual ∼1 nm diameter nanocavity is defined by the interlocking of four nanogrids. The interlocking nanogrids are of the same chirality, which is associated with the fact that exclusively homochiral species match. In contrast, there is no smooth joining of *R*- and *S*-type nanogrids; it is obstructed by the tilt angle between the mirror-symmetric species implying a geometric mismatch (in analogy to stereochemistry-driven hydrogen-bonded homochiral supramolecular assemblies, cf. ref 8). As a striking consequence chirality is bestowed to the entire nanocavity arrays. Accordingly, as shown in Figure 2a, two domains exist on the surface which are mirror images of each other, whereby the symmetry axis is given by the high symmetry [011] direction of the

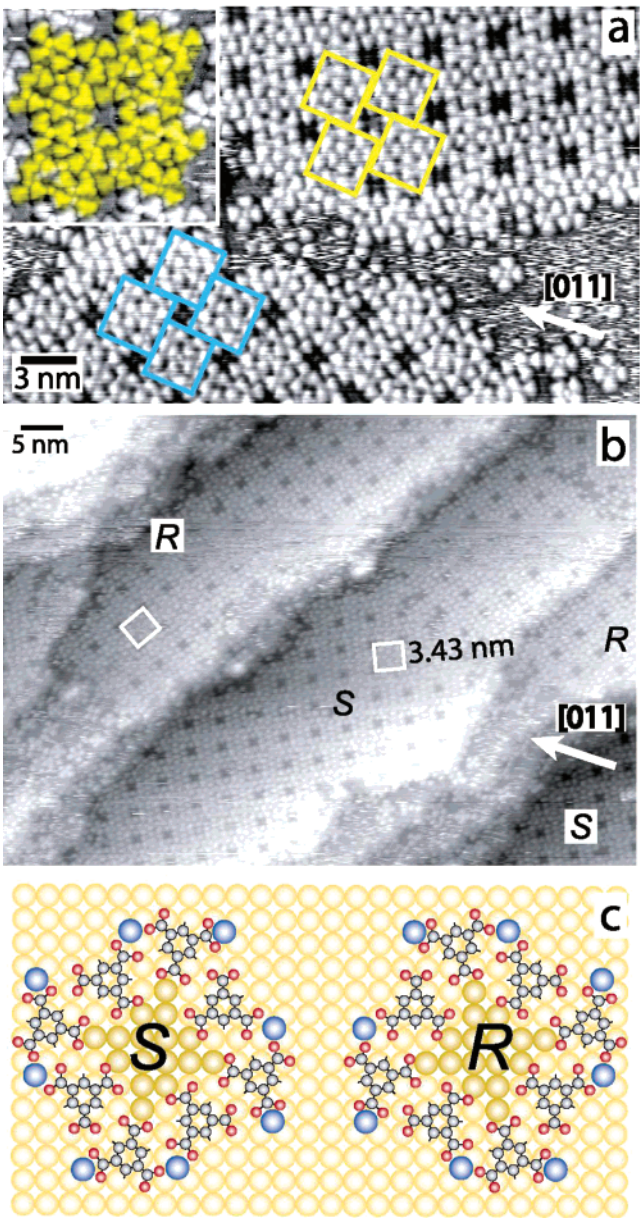

Figure 2. (a) Formation of extended nanocavity arrays triggered by 400 K annealing. Two homochiral domains are assembled consisting of pure enantiomers (marked by color rectangles, coding as in Figure 1). The inset is a high-resolution image of a *S*-type nanocavity, which is surrounded by eight TMA molecules. The nanogrid arrangement belongs to the p4 symmetry group. (Fe coverage: 0.06 ML; TMA coverage: 0.8 ML). (b) Highly organized homochiral domains cover the entire surface at saturation coverage. Enantiopure domains labeled *R* and *S* comprise homochiral nanogrids. Unit cells of both domains are indicated. (Fe coverage: 0.06 ML; TMA coverage: 0.8 ML). (c) Tentative model of nanocavities from STM topography, where the *S* (*R*) nanocavity is assembled from *S* (*R*) motifs. The central opening (where the copper atoms are colored slightly darker) is functionalized by the eight surrounding carboxylate groups. It represents a chiral host for chiroselective adsorption of guests ar enantioselective heterogeneous catalytic processes.

Cu(100) substrate (marked by the arrow in Figure 2a). In matrix notation the corresponding unit cells read

$$\begin{bmatrix} 12 & 6 \\ -6 & 12 \end{bmatrix}$$

for *R* and

$$\begin{bmatrix} 6 & 12 \\ -12 & 6 \end{bmatrix}$$

for *S* type meshes, respectively. The assembly of the nanocavity arrays is thus chiroselective or chiroinductive, i.e., in their evolution only the building blocks with the appropriate chirality are assembled or alternatively the chiral signature of the incorporated material is induced by already existing arrangements. The net result is in either case that enantiopure domains evolve with a distinct higher level of organization as the preceding racemic mixture of isolated nanogrids.

Elucidating the self-assembly kinetics at the employed temperatures (350−400 K) is unattainable by our instrument because the relevant time scale of the kinetic processes are beyond the temporal resolution of the STM (>5 s per image frame). With the present data and instrumental limitations the pathways of the assembly can unfortunately not be conclusively unraveled. However, it is important to note that 400 K annealing is crucial to activate the surface diffusion of the multinuclear nanogrids. It is also important to note that both an appreciable concentration of Fe atoms and TMA molecules with the given concentration ratio and the thermal activation are prerequisites for network formation. That is, key factors in the encountered scenario include balanced constitutents' concentration, thermal motion, reorganization of mononuclear complexes or multinuclear nanogrids, and energy barriers to be overcome for association.

Large-scale STM data (cf. Figure 2b) reveal that at saturation coverage a well-ordered layer comprising the supramolecular motif readily covers the entire surface. The respective homochiral single domains were found to be robust (thermal stability up to 450 K) and to be up to 50 nm wide, extending over entire substrate terraces. As expected there is an equal distribution of *R*- and *S*-type domains. The inset in Figure 2a demonstrates furthermore that each nanocavity is enclosed by eight TMA molecules, which account for an opening with an inner diameter of ∼1 nm. Since each TMA vertex carries a carboxylate group, in total eight COO ligands surround a single cavity. A tentative model of the nanocavities is shown in Figure 2c (the orientation of the carboxylate groups cannot be conclusively determined on the basis of STM data, and they may rotate out of the molecular plane). The distinct size, shape, and chemical functionality make the nanocavity arrays a promising candidate to be employed as host system for the selective adsorption of molecular guests. In addition to its chemical functionality the homochiral nature of the nanocavities is of great interest for enantioselective recognition and asymmetric catalysis.

Conclusions

Our observations demonstrate that the hierarchical assembly of robust metal−organic architectures at surfaces can be followed at the single-molecule level and provides a novel rationale for the fabrication of highly organized supramolecular materials. This extremely versatile approach implies the potential to construct surface-supported nanocavity coordination arrays with programmed size, shape, and functionality by the appropriate choice of the employed constituents. Moreover, the distinct arrangement of metal centers and organic molecules in these systems accounts for multifunctional nanostructured templates.

Experimental Section

TMA molecules and iron atoms were sequentially deposited on a Cu(100) single-crystal surface in a standard ultrahigh vacuum chamber with a base pressure of $\sim 3 \times 10^{-10}$ mbar. In situ STM experiments employing the constant current mode were performed at room temperature. The Cu(100) surface was cleaned by repeated cycles of Ar^+ sputtering and subsequent annealing to 800 K, whereupon flat terraces of up to 100 nm width separated by monatomic steps were obtained. TMA (99+%, Sigma-Aldrich Chemie GmbH) was deposited by organic molecular beam epitaxy (OMBE) from a Knudsen-cell type evaporator, held at 463 K during deposition. The TMA monolayer (ML) is defined as the substrate fully covered by a dense-packed arrangement of flat-lying species, which accounts for 0.046 TMA per a_0^2 ($a_0 = 2.55$ Å is the nearest-neighbor spacing of copper atoms in the (100) plane). Fe atoms were evaporated using an e-beam heating evaporator. One monolayer of Fe corresponds to 1 Fe atom per a_0^2. The ratio of Fe atoms to TMA molecules employed for the preparation of extended networks is typically 1.6, which is appreciably higher than the stoichiometric ratio derived from the structure model for ideal coordination networks (9:16). This difference is attributed to the effective loss of Fe atoms in other processes, for instance, Fe island formation, decoration of steps, step and surface alloying with the Cu substrate, that is not the entire amount of deposited Fe is incorporated in the nanocavity arrays. In particular we observed that with increasing annealing temperature higher Fe-to-TMA ratios have to be used, which is associated with enhanced Fe loss for higher temperatures. This is in agreement with the fact that surface intermixing becomes generally more pronounced with increasing temperature.

Acknowledgment. Financial support from the *Schweizerischer Nationalfonds zur Förderung der wissenschaftlichen Forschung* (H.S.) and the *Volkswagenstiftung* is gratefully acknowledged.

JA0362353